JOURNAL OF PHYSICAL ORGANIC CHEMISTRY
J. Phys. Org. Chem. 2006; **19:** 157–166
Published online 23 January 2006 in Wiley InterScience (www.interscience.wiley.com). DOI: 10.1002/poc.1014

Analysis of interaction modes in calix[4]arene–levofloxacin complexes by quantum methods

Alexandrine Lambert,[1] Jean-Bernard Regnouf-de-Vains,[2] Daniel Rinaldi[1] and Manuel F. Ruiz-Lopez[1]*

[1]Equipe de Chimie et Biochimie Théoriques, UMR CNRS-UHP No. 7565, Université Henri Poincaré, Nancy I, BP 239, 54506 Vandoeuvre-lès-Nancy Cedex, France
[2]GEVSM, UMR CNRS-UHP No. 7565, Falculté de Pharmacie Université Henri Poincaré, Nancy I, 5 rue Albert Lebrun BP 80403, 54000 Nancy, France

Received 20 May 2005; revised 20 September 2005; accepted 19 October 2005

ABSTRACT: Host–guest interactions between chiral calix[4]arenes and the antibiotic levofloxacin are analyzed on the basis of quantum mechanical calculations at the density functional (for model systems) and semi-empirical levels. The calix[4]arene macrocycle carries two (+)-isomenthyl groups attached to opposing phenyl groups at the lower rim and different substituents (R = H, CH_3, tBu, CH_2CHCH_2, $COCH_3$ and NO_2) are considered at the upper rim. Nitro derivatives are expected to form ionized complexes whereas the other derivatives should form neutral complexes with a very low stability. Copyright © 2006 John Wiley & Sons, Ltd.

KEYWORDS: calixarenes; levofloxacin; host–guest complexes; chiral recognition; quantum mechanics

INTRODUCTION

Quinolones are synthetic molecules exhibiting antibacterial properties.[1–6] They act by inhibiting two fundamental enzymes, topoisomerase II or DNA-gyrase, and topoisomerase IV, both involved in cell division processes. The first member of this family, nalidixic acid, was synthesized in 1962[1] and exhibited antibacterial activity towards Gram-negative bacteria. In the 1970s, other quinolones such as piromidic acid and flumequine were developed that had increased Gram-negative and systemic activity. Flumequine possesses a fluor atom in position 9 and its activity towards Gram-negative bacteria is ten times higher than that of nalidixic acid. In addition, it is also active on Gram-positive bacteria. More recently, the combination of a fluor atom in position 6 and a piperazine substituent in position 7 has been found to confer quite interesting properties to these compounds and has led to a new generation of quinolone antibiotics, the so-called fluoroquinolones.[5] Since the discovery of norfloxacin many other molecules[2,3,7] have been developed that are of current therapeutic use, such as ciprofloxacin, ofloxacin and levofloxacin.

In fact, ofloxacin, as flumequine, is provided as a racemic mixture. Levofloxacin (Lfx) is the corresponding *levo*-enantiomer, S-(−)-ofloxacin (see Fig. 1). Previous work has shown that the activity of Lfx is much higher than that of the *dextro*-enantiomer, R-(+)-ofloxacin, and approximately twice times that of the racemate.[7,8] However, in spite of their different antibacterial activity, both enantiomers display similar toxicities. Following recommendations of regulatory authorities for chiral drugs, only the active enantiomer of a chiral drug should reach the market and therefore efforts have been made to develop selective separation methods of ofloxacin enantiomers. There are several analytical methods for the direct chiral separation of ofloxacin, including capillary electrophoresis with various cyclodextrins as chiral selector.[9–12]

Another promising route is offered by the use of calixarene derivatives, which has the advantage of being quite flexible from a synthetic point of view compared with cyclodextrins. Calixarenes display selective complexation properties that make them suitable for a large number of applications, such as luminescent probes, nuclear waste treatment or molecular sensors.[13] Until now calixarenes have not been much used as chiral selectors, but recent works have reported encouraging results. For instance, Lynam *et al.*[14] have synthesized propanol amide derivatives of *p*-allylcalix[4]arene that behave as a selector of amines due to their shape and chirality. Zheng and Zhang[15] have shown that calixarenes bearing α,β-aminoalcohol groups are efficient chiral selectors of carboxylic acids. For most of the studies reported, chiral calix[4]arenes are obtained by attaching chiral residues at the lower rim[14–20] or upper rim.[21]

A rational design of new molecules with improved properties may be simplified significantly by the use of theoretical chemistry methods. However, there are two main difficulties. First, host–guest interaction energies need to be computed accurately because significant

**Correspondence to:* M. F. Ruiz-Lopez, Equipe de Chimie et Biochimie Théoriques, UMR CNRS-UHP No. 7565, Université Henri Poincaré, Nancy I, BP 239, 54506 Vandoeuvre-lès-Nancy Cedex, France.
E-mail: manuel.ruiz@cbt.uhp-nancy.fr

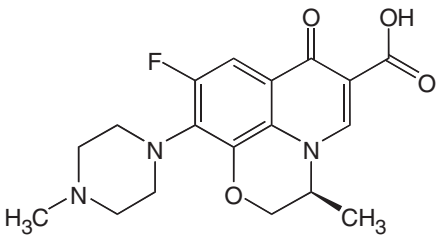

Figure 1. Levofloxacin (Lfx) structure

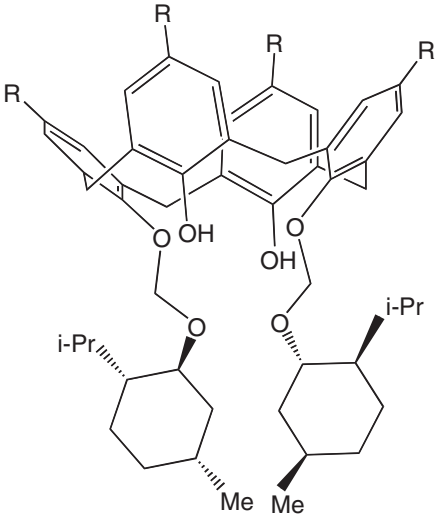

Figure 2. Schematic representation of the calix[4]arene molecules considered in the present work (R = H, CH_3, tBu, CH_2CHCH_2, $COCH_3$ and NO_2)

enantioselectivities may be achieved for small energy differences (owing to the exponential form of the Boltzmann factor). In principle, this can be done through the use of *ab initio* techniques but system size limits their use. Second, due to the flexibility of the host–guest complexes, a large set of structures representing a suitable sampling of the configuration space must be considered. To this end, statistical simulation techniques (such as Monte Carlo or molecular dynamics) may be employed but in general they are based on empirical force fields that do not provide very accurate interaction energies. Combined quantum mechanics and molecular mechanics methods (QM/MM) and *ab initio* molecular dynamics (AIMD) represent the most promising approaches in this field. Investigations at this level still represent a considerable amount of computational time and thus before they are undertaken it is essential to elucidate the basic interaction mechanisms operating between the host and guest molecules.

In the present work, we investigate complex formation between a series of chiral calix[4]arene derivatives and the antibiotic Lfx. The calixarene macrocycle carries two (+)-isomenthyl substituents at the lower rim attached to opposite phenyl groups (Fig. 2). They define a chiral environment for the complexation site, constituted by the residual hydroxyl groups. Their acidic behavior, even modest, is expected to favor interactions with the amino groups of the quinolone species. This molecule (R = tBu) has been synthesized in our group and host–guest complexes with piperazine-bearing quinolones, particularly Lfx, will be studied experimentally very soon. The present work aims at analyzing a number of fundamental questions: the stability of the complexes, the mechanism of interaction and the effect of substituents in the upper rim.

COMPUTATIONS

Because of computational time limitations, previous theoretical studies on calix[4]arene systems and complexes have been made essentially at the molecular mechanics level (Refs. 22–30 and references cited therein). A few systems have been investigated through semi-empirical quantum chemical techniques. The properties of calix[4]arenes in the *cone* conformation have been investigated with special attention paid to the equilibrium geometry,[31,32] hydrogen bonds[33] and charge delocalization in polyanions.[22] Semi-empirical calculations have been used also to investigate the influence of conformation on second-order non-linear optical properties of calix[4]arenes[34,35] and to assess the importance of π–π interactions in C60-fullerene/*p-t*-butylcalix[8]arene 1:1 adducts.[36] Molecular dynamics simulations based on combined AM1/TIP3P potentials have been applied to analyze the role of electronic polarization on the liquid phase affinity of calixarene-crown-ethers towards alkali cations.[37] The interaction of alkylammonium ions and quinone derivatized calix[4]-arenes was studied by Chung *et al.*[38] More recently, AM1 calculations were performed on *p-t*-butylcalix[4]arene-crown-6 and some of its alkylammonium cation complexes, to estimate the binding energy and enthalpy of formation of such compounds.[39]

The large computational resources required to evaluate the energy and structure of calixarenes have prevented *ab initio* or density functional treatments until recently. Thus, studies on hydroxylated calix[4]arene,[40] thiacalix[4]arene,[41] tetramethoxy-calix[4]arene[42] and cation–π interactions[43] have been published. Finally, tetramethoxy-calix[4]arene and 1,3-alternate-dimethoxy-calix[4]arene-crown-6 complexes with alkali cations have also been reported.[44]

In the present work, we have chosen to perform two types of studies. First, density functional theory (DFT) calculations have been carried out for a series of model complexes. Then, semi-empirical calculations have been made for the whole system. Semi-empirical approaches are not expected to provide very accurate results for the absolute complexation energies but they allow the main trends along a chemical family to be obtained. Furthermore the combination of semi-empirical and

DFT calculations for model systems has allowed us to estimate the error made in the semi-empirical computations for real systems. This is connected to the computational strategy of the ONIOM method,[45] as detailed below.

The DFT calculations have been made using the hybrid exchange-correlation functional B3LYP and the 6–31 + G* basis set. The use of polarization and diffuse functions on heavy atoms has been considered as crucial for a good description of ion-pair complexes. The B3LYP method seems to be a good compromise between reliability and computational cost, as demonstrated by many examples.[46] Semi-empirical computations have been done using the PM3 method. The geometry of all systems has been optimized in vacuum and solution. The solvent effect was taken into account by employing a dielectric continuum model. We have used the approach developed in our group, which assumes a molecular-shaped cavity and a multicentric multipolar expansion[47] of the reaction field. We have considered a polar medium with dielectric constant $\epsilon = 47$. This value corresponds to dimethyl sulfoxide (DMSO), a typical solvent used in experimental studies. However, one should note that in dielectric continuum models the increase of the solvent reaction field with the dielectric constant becomes rather slow for ϵ beyond 15–20. In other words, the trends described in our calculations should still be appropriate for other polar media, although the expected overall effect would be slightly larger or smaller depending on its dielectric constant. In all cases, we have used the Gaussian 98 code.[48]

The choice of the initial structure of the calix[4]arene molecule and of the calix[4]arene–Lfx complexes was made as follows. An NVT molecular dynamics (MD) simulation of the calix[4]arene was carried out using the AMBER force field[49] and the Discover program of the Insight II 95.0 software (Biosym Technologies, San Diego, SA, USA, 1995). The initial structure was constructed with a calix[4]arene (R = tBu) in cone conformation, which was shown to be the most stable conformation in previous studies.[22,25] The simulation consisted of an equilibration phase of 50 ps (0.2 fs time step for a total of 250 000 steps) and a data acquisition phase of 400 ps at 300 K. Analysis of the results showed structural features that are comparable to previous studies of the same type. Thus, there are two different average oxygen–oxygen distances for atoms in opposite phenol rings (3.7 Å and 5.2 Å), as also reported for a similar calix[4]arene unsubstituted at the lower rim.[23] Noteworthy, in our case, the most favorable conformation of the calixarene (85% of the total simulation time) displays the smallest oxygen–oxygen distance for the phenol groups bearing the isomethyl groups. This structural arrangement allows the hydrogen atoms of the hydroxyl groups to form hydrogen bonds with the oxygen atoms attached to the isomenthyl groups.

From the simulation, a set of 200 configurations was selected by steps of 2 ps. For each configuration, full PM3 geometry optimization was carried out. The lowest energy conformation is represented in Fig. 3. Other less-stable conformations lie within an energy range of roughly 18 kcal mol^{-1} (1 kcal = 4.184 kJ). The PM3 calculations confirm the structural features described above for oxygen–oxygen distances and hydrogen bonds. In particular, for 81% of the optimized configuration set the shortest oxygen–oxygen distance corresponds to the phenol groups bearing the isomenthyl groups. The four tBu groups were then replaced by H, CH_3, CH_2CHCH_2, $COCH_3$ or NO_2 and the corresponding calix[4]arene geometries were completely relaxed at the PM3 level.

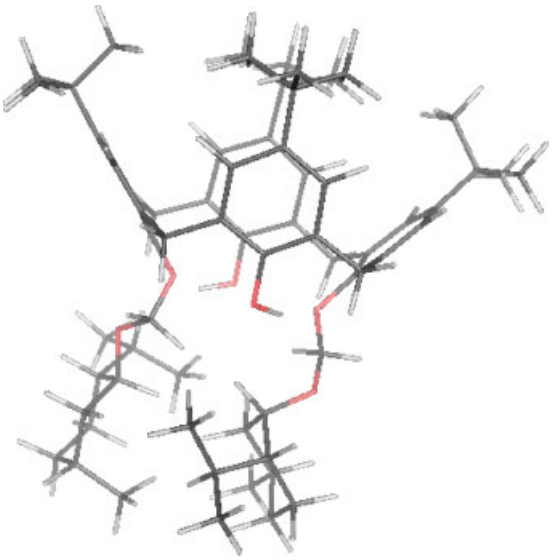

Figure 3. Optimized structure for the (+)-isomenthyl *t*-butylcalix[4]arene derivative studied here using the PM3 method

Starting from the optimized structure of the calixarene, Lfx was docked in the macrocycle. Several interaction modes were envisaged, as explained below. Full PM3 geometry optimizations were carried out for several trial initial configurations although only the most stable one for each interaction mode will be considered in the following. Due to the flexibility of the complex, a more realistic study would require a rigorous statistical treatment to be performed. However, as explained in the introduction, the present work aims to provide a qualitative description of the host–guest interaction that is needed before computationally demanding QM/MM or AIMD simulations are carried out.

RESULTS

Choice of interaction modes

Quinolones possess acid and amino functional groups. Accordingly, they may exist as neutral, cationic, anionic or zwitterionic species, the actual ionization state of the molecule depending on the pH. Predicting the ionization

state in a particular solvent and pH is an intricate question that goes beyond the present work objectives. Nevertheless, it is an important problem and will be considered in forthcoming studies. Note that spontaneous deprotonation of Lfx in DMSO seems unlikely, because typical p*Ka* values of carboxylic acids in this solvent are of the order of 12 units.[64]

For the neutral Lfx molecule considered here, two major interacting modes can be invoked: the calixarene phenol (proton donor) and an amino Lfx group (proton acceptor); and the calixarene phenol (proton acceptor) and the carboxylic Lfx group (proton donor). Exploratory calculations showed that the latter is less stable than the former by roughly 5 kcal mol^{-1} and has not been considered further in this paper.

The interaction of calixarene derivatives with neutral amines, ammonium ions and amino acids has been considered in some experimental[38,50–56] and theoretical reports.[28,57] The interaction with quaternary ammonium ions has attracted much interest due to the biological relevance of similar catio–π interactions in the recognition of acetylcholine by the enzyme acetylcholinesterase,[58,59] but the interaction with neutral amines has been broadly considered too (for a review see Ref. 60). Bauer and Gutsche[51] showed that aliphatic amines interact strongly in polar solvents with calix[4]arenes to form complexes that were thought to involve proton transfer and ion pairing. Indeed, the p*Ka* values for phenols in calixarenes are below those for the corresponding phenols, allowing the formation of salts with amines.[61] Nachtigall *et al.*[53] described the crystal structure of calix[4]arene piperidinium salts in which the calixarene adopts a cone conformation and the ions are held together by strong hydrogen bond interactions (oxygen–oxygen distances are 2.527 Å and 2.494 Å). Similar results[62] were obtained for other amines, including piperazine, a functional group in Lfx. Recent experimental studies on the interaction of mono-*p*-nitro-calix[4]arene[63] with Lfx have been carried out in our group. A UV–visible titration has been carried out in solvents of different polarity, specifically CH_2Cl_2, CH_3COCH_3, CH_3CN and DMSO. In polar solvent, the titration exhibits (J.B. Regnouf-de-Vains, unpublished results) an absorption band at 438 nm, which is characteristic of the formation of a *p*-nitro phenate species.

The above remarks incited us to investigate the formation of neutral and ionized complexes in which the macrocycle acts as proton donor. Because of steric hindrance, only the Lfx amino group carrying a methyl group is expected to interact with the phenol. The following chemical equilibria will be considered:

$$\text{CalixOH} + \text{Lfx} \rightleftharpoons \text{CalixOH}\cdots\text{Lfx} \quad (1)$$

$$\text{CalixOH} + \text{Lfx} \rightleftharpoons \text{CalixO}^- + \text{HLfx}^+ \quad (2)$$

$$\text{CalixO}^- + \text{HLfx}^+ \rightleftharpoons \text{CalixO}^-\cdots\text{HLfx}^+ \quad (3)$$

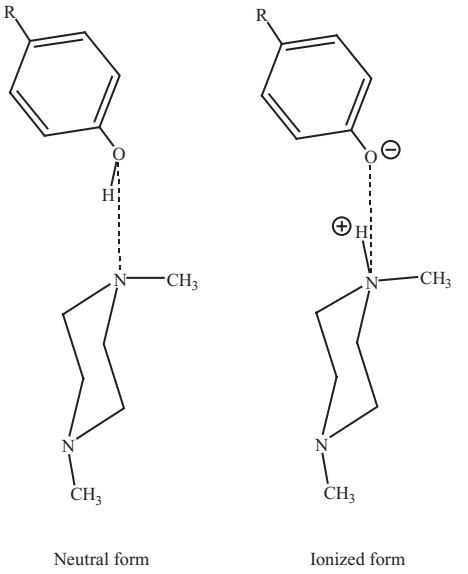

Figure 4. Schematic representation of model complexes of *p*-monosubstituted phenol (*p*-R-PhOH)–1,4-dimethylpiperazine (DMP)

Study of model systems at the DFT and *ab initio* levels

Before considering the calix[4]arene–Lfx systems, we have considered the interaction in model compounds, namely *p*-monosubstituted phenol (*p*-R-PhOH) and 1,4-dimethylpiperazine (DMP) (Fig. 4).

The DFT calculations have been made for R = H, $COCH_3$ and NO_2. Full geometry optimization of the neutral systems (*p*-R-PhOH and DMP), neutral complex (*p*-R-PhOH$\cdots$DMP), ionized systems (*p*-R-PhO^- and $HDMP^+$) and ionized complex (*p*-R-$PhO^-\cdots HDMP^+$) has been done in gas phase and solution. However, the ionized complex has been obtained only for the substituted derivatives when one takes into account the stabilizing effect due to the solvent. In the other cases, the proton is transferred to the phenol oxygen atom during the optimization procedure to obtain the neutral complex. Some geometrical parameters for the optimized structures are summarized in Table 1, and relative energies with respect to the separated neutral molecules are gathered in Table 2. A few remarks can be made concerning the hydrogen bond distances: they are shorter in solution than in gas phase; substitution of the phenol leads to a decrease in bond distance; the hydrogen bonds are much shorter for ionized complexes (by as much as 0.1 Å in the case of $R = NO_2$); and the N–O–H angles are rather small (about 6–7° in neutral complexes) and decrease through proton transfer (3–4° in ionized complexes).

As shown in Table 2, complexation and ionization energies decrease in the order $H > COCH_3 > NO_2$. This trend is consistent with the increasing acidity of the phenol derivatives (experimental p*Ka* in water: 9.82, 8.05 and 7.15 for R = H, $COCH_3$ and NO_2, respectively).

Table 1. Geometry of neutral and ionized phenol–DMP complexes as optimized in gas phase and DMSO solution at the B3LYP/6–31 + G* level ($d_{X\text{-}H}$ represents the hydrogen bond length: X = N for neutral complexes; X = O for ionized complexes)

		Gas phase			Solution ($\varepsilon = 47$)		
R	Complex	$d_{N\text{-}O}$ (Å)	$d_{X\text{-}H}$ (Å)	$\alpha_{N\text{-}O\text{-}H}$ (degrees)	$d_{N\text{-}O}$ (Å)	$d_{X\text{-}H}$ (Å)	$\alpha_{N\text{-}O\text{-}H}$ (degrees)
H	Neutral	2.801	1.818	8.5	2.760	1.762	7.5
$COCH_3$	Neutral	2.767	1.779	8.6	2.727	1.717	6.6
$COCH_3$	Ionized	—	—	—	2.592	1.493	3.0
NO_2	Neutral	2.740	1.746	8.5	2.671	1.647	7.0
NO_2	Ionized	—	—	—	2.619	1.084	4.4

Table 2. The B3LYP/6–31 + G* energies[a] for complexation and ionization processes of the phenol + DMP systems in a vacuum and DMSO solution

	Gas phase			Solution ($\varepsilon = 47$)		
R	Neutral complex	p-R-PhO^- + $HDMP^+$	Ionized complex	Neutral complex	p-R-PhO^- + $HDMP^+$	Ionized complex
H	−9.72	112.45	—	−7.52	12.94	—
$COCH_3$	−10.86	97.09	—	−7.82	5.33	−5.49
NO_2	−12.12	86.78	—	−9.24	−0.61	−11.03

[a] Values (in kcal mol^{-1}) are relative to the separated neutral molecules.

Ionization energies are, as expected, much smaller in solution than in the gas phase, but only in the case of the most acidic species R = NO_2 is the ionization energy is negative in solution. The formation of a neutral complex is not favored by the solvent effect, whereas the formation of an ionized complex is slightly favored in the case of $COCH_3$ and strongly favored in the case of NO_2. As a result, for the latter substituent the ionized complex is predicted to be the most stable species in solution.

Study of the model systems at the PM3 level

The PM3 calculations have been made for a series of model systems with R = H, CH_3, tBu, CH_2CHCH_2, $COCH_3$ and NO_2. As in B3LYP calculations, neutral systems (p-R-PhOH and DMP), neutral complexes (p-R-PhOH···DMP), ionized systems (p-R-PhO^- and $HDMP^+$) and ionized complexes (p-R-PhO^-···$HDMP^+$) have been fully optimized in gas phase and in solution. Some geometrical parameters are presented in Table 3. The energies of these systems relative to the separated neutral molecules are summarized in Table 4. If one compares the PM3 results for the neutral complexes with the B3LYP calculations (R = H, $COCH_3$, NO_2) one sees that PM3 reproduces the main trends outlined above. In particular, hydrogen bonds display a similar geometrical arrangement ($d_{N\text{-}H}$ slightly larger than 1.8 Å; $\alpha_{N\text{-}O\text{-}H}$ about 7–8°) and a comparable solvent effect (both hydrogen bond distances and angles decrease in solution).

Table 3. Geometry of neutral and ionized phenol–DMP complexes as optimized in gas phase and DMSO solution at the PM3 level ($d_{X\text{-}H}$ represents the hydrogen bond length: X = N for neutral complexes, X = O for ionized complexes)

		Gas phase			Solution ($\varepsilon = 47$)		
R	Complex	$d_{N\text{-}O}$ (Å)	$d_{X\text{-}H}$ (Å)	$\alpha_{N\text{-}O\text{-}H}$ (degrees)	$d_{N\text{-}O}$ (Å)	$d_{X\text{-}H}$ (Å)	$\alpha_{N\text{-}O\text{-}H}$ (degrees)
H	Neutral	2.803	1.845	7.2	2.788	1.829	7.0
H	Ionized	—	—	—	2.693	1.625	0.0
CH_3	Neutral	2.803	1.846	7.2	2.789	1.830	7.1
CH_3	Ionized	—	—	—	2.685	1.615	2.2
tBu	Neutral	2.803	1.846	7.2	2.789	1.831	7.1
tBu	Ionized	—	—	—	2.686	1.612	1.1
CH_2CHCH_2	Neutral	2.801	1.845	7.2	2.788	1.830	7.0
CH_2CHCH_2	Ionized	—	—	—	2.683	1.614	2.7
$COCH_3$	Neutral	2.795	1.836	7.0	2.780	1.819	6.7
$COCH_3$	Ionized	2.660	1.552	3.9	2.704	1.647	1.7
NO_2	Neutral	2.782	1.820	6.8	2.768	1.804	6.6
NO_2	Ionized	2.682	1.603	3.4	2.718	1.670	2.1

Table 4. The PM3 energies[a] for the interaction between *p*-substituted phenol and DMP in a vacuum and DMSO solution

	Gas phase			Solution ($\varepsilon = 47$)		
R	Neutral complex	*p*-R-PhO$^-$ + HDMP$^+$	Ionized complex	Neutral complex	*p*-R-PhO$^-$ + HDMP$^+$	Ionized complex
H	−4.58	136.41	—	−2.75	36.78	25.79
CH_3	−4.54	136.00	—	−2.66	37.14	26.15
tBu	−4.50	135.40	—	−2.49	37.43	27.12
CH_2CHCH_2	−4.93	134.47	—	−2.77	36.87	26.04
$COCH_3$	−5.41	123.41	29.37	−3.17	30.49	21.83
NO_2	−6.38	109.00	23.83	−3.16	22.34	15.55

[a] Values (in kcal mol^{-1}) are relative to the separated neutral molecules.

For ionized complexes, the most striking result is that PM3 predicts stable structures in the gas phase, in contrast to B3LYP. However, for the structures in solution PM3 predicts structures in reasonably good agreement with B3LYP ($d_{\text{O-H}}$ slightly larger than 1.6 Å; $\alpha_{\text{N-O-H}}$ about 1–4°).

Complexation energies for neutral complexes are underestimated in the case of PM3 (by about 5–6 kcal mol^{-1}), although this method reproduces well the substituent and the solvent effect on this quantity. Relative energies for ionized systems (*p*-R-PhO$^-$ + HDMP$^+$) and for ionized complexes (*p*-R-PhO$^-\cdots$ HDMP$^+$) exhibit much larger deviations with respect to B3LYP. Clearly, PM3 strongly underestimates the stability of these species. This large difference between B3LYP and PM3 must be related to errors found with semi-empirical methods when computing intrinsic acidity and basicity properties of molecules. Consider, for instance, the processes:

$$\text{PhOH} \rightarrow \text{PhO}^- + \text{H}^+ \quad (4)$$

$$\text{DMP} + \text{H}^+ \rightarrow \text{HDMP}^+ \quad (5)$$

The PM3-computed enthalpies for reactions (4) and (5) are 331.15 and −194.74 kcal mol^{-1}, respectively. The corresponding values at the B3LYP level are 350.98 and −238.52 kcal mol^{-1}. As shown, the gas-phase acidity of phenol is overestimated by PM3 whereas the basicity of piperazine is underestimated. The errors are partially compensated when one considers the whole acid–base reaction:

$$\text{PhOH} + \text{DMP} \rightarrow \text{PhO}^- + \text{HDMP}^+ \quad (6)$$

but one still finds substantial deviations, and the predicted PM3 value in Table 4 (136.41 kcal mol^{-1}) is much higher than that for B3LYP in Table 2 (112.45 kcal mol^{-1}). The difference amounts to roughly 24 kcal mol^{-1}. Hence, PM3 does not yield reliable ionization energies, which represents an important shortcoming if one aims at using this method to describe much larger systems. Nevertheless, the ionization energy error in reaction (6) may be considered as a systematic deviation, i.e. one expects a similar error for the ionization reaction between different phenol and piperazine derivatives and, in particular, for the calix[4]arene and Lfx systems envisaged below. Moreover, analysis of the data in Tables 2 and 3 shows that an equivalent error is expected when evaluating the relative stability of ionized complexes. Indeed, one finds a linear correlation between the PM3 and B3LYP results for the relative energies of *p*-R-PhO$^-$ + HDMP$^+$ and *p*-R-PhO$^-\cdots$HDMP$^+$, such that (in kcal mol^{-1}) $\Delta E(\text{PM3}) = 25.2 + 0.989\,\Delta E(\text{B3LYP})$, with $R = 0.999$ (this correlation is obtained by using values from Tables 2 and 3 and including both gas-phase and solution calculations).

In order to make a more detailed comparison between PM3 and B3LYP, we have analyzed the potential energy surface for proton transfer in the model complex phenol–piperazine. We have arbitrarily chosen as distinguished coordinates the NO and the NH distances, which are varied by steps of 0.2 Å. For given NO and NH distances, the other geometrical parameters are relaxed at the PM3 level and this is followed by single-point calculations at the B3LYP level. Note that this choice would not necessarily be a good one in a theoretical study on proton transfer kinetics, which should take into account the small relaxation time of the proton with respect to the other geometrical coordinates.

The potential energy curves are plotted in Fig. 5. Results are given in both gas phase and solution. One may note that both methods always predict an energy minimum in the case of neutral complexes, whereas only some energy minima are predicted for ionized complexes. Qualitatively, the results predicted by these methods are comparable but there are two main differences: PM3 displays a greater trend to get stationary points for short NH distances, i.e. for ionized complexes (consider, for instance, the curves in solution for N–O = 2.7 Å); and the relative energy between neutral and ionized complexes is substantially method dependent, with PM3 underestimating the relative stability of ionized structures by 20–25 kcal mol^{-1}. The first point explains why PM3 predicts some ionized complexes for which no B3LYP energy minimum could be found. The second point confirms the systematic trend of PM3 to underestimate

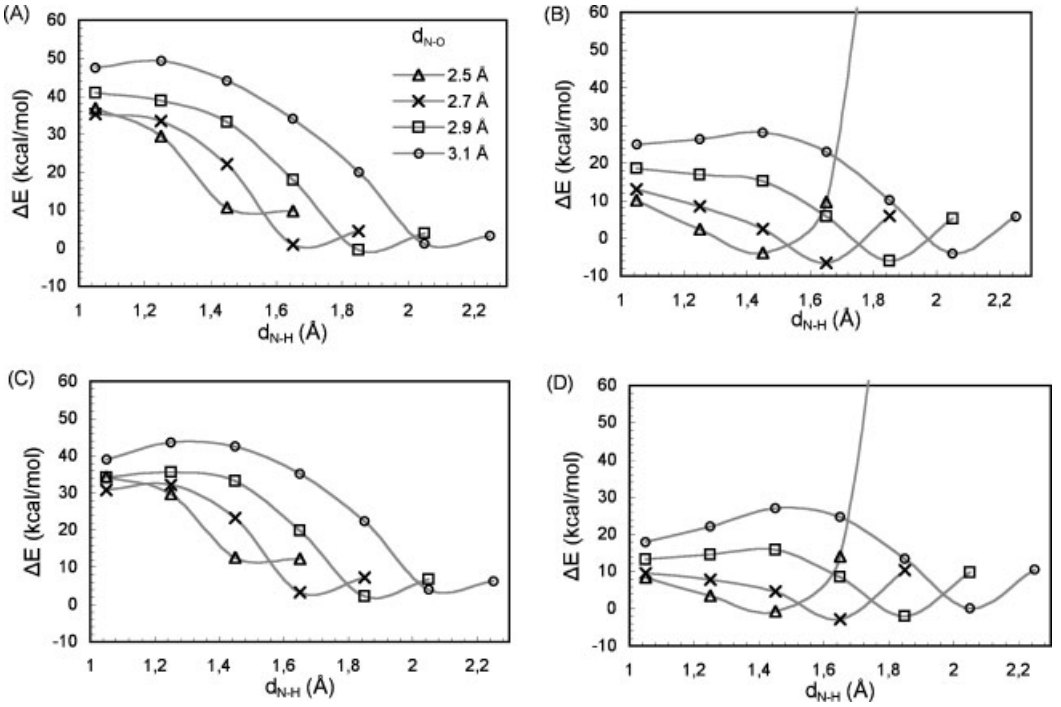

Figure 5. Potential energy surfaces for proton transfer in the model phenol–piperazine complex. We have chosen as distinguished coordinates the NO and the NH distances. Each curve corresponds to an NO distance, as indicated. Gas-phase calculations correspond to curves A (PM3) and B (B3LYP). Solvent calculations correspond to curves C (PM3) and D (B3LYP). ΔE is given relative to the neutral separated molecules

proton transfer between phenol and piperazine derivatives. Note that, as expected, the interaction with the solvent stabilizes the ion-pair complexes.

The previous analysis shows that PM3 calculations for ionized systems and ionized complexes need to be corrected. The ONIOM method[45] has often been used to this end in the study of complex systems. Basically, a sub-system (the model) is defined and described using both low- and high-level computational methods, whereas the whole system is treated at the low level only. Then, the estimated high-level energy of the real system is simply given by the energy difference E(high, real) $-$ E(low,real) $+$ [E(high,model) $-$ E(low,model)]. Although the ONIOM approximation has proved to be quite useful, it needs to carry out a high-level calculation for the model and can become costly if many systems are to be studied. Indeed, when one is interested in a homogeneous chemical series, as in our case, it can be more efficient to make a systematic correction to low-level computations for the real systems. We propose here to use the equation:

$$\Delta E_{\text{corr}}^{\text{PM3}} = \Delta E^{\text{PM3}} - 24\,\text{kcal mol}^{-1} \qquad (7)$$

for systems involving ionized species. The equation is derived for reaction (6) but is similar to the linear fitting equation presented above. Moreover, a test calculation (below) shows that this expression is also suitable for the calixarene–Lfx system. The corrected energy $\Delta E_{\text{corr}}^{\text{PM3}}$ should be much more realistic than the standard PM3 result. This correction will be used for the calixarene–Lfx systems below.

Study of calix[4]arene–levofloxacin complexes

As in model systems, we consider R = H, CH_3, tBu, CH_2CHCH_2, $COCH_3$ and NO_2. In all cases, energy minima have been obtained for neutral and ionized complexes. The corresponding geometries are presented in Table 5 (for the sake of simplicity, only calculations in solution are presented). The optimized complexes for the tBu derivative are shown in Fig. 6. The structural parameters clearly show that for the neutral complexes there are no effective hydrogen bonds between the host and guest molecules. On the contrary, for the ionized complexes, one predicts short hydrogen bonds similar to those found for the model complexes (although the bond angles $\alpha_{\text{N-O-H}}$ are slightly larger).

Complexation and ionization energies are summarized in Table 6. Values are given relative to the separated neutral molecules. Note that Eqn (7) is used to correct the relative energies of systems involving ionized species. As mentioned, we have carried out a test calculation in order to verify the suitability of such an equation in this case. The PM3 and DFT energy calculations (B3LYP/6–31 + G* level) have been made for the neutral and ionized complexes of the calix[4]arene

Table 5. Geometry of neutral and ionized calix[4]arene–levofloxacin complexes as optimized in DMSO solution ($\varepsilon = 47$) at the PM3 level

	Neutral complex			Ionized complex		
R	$d_{N\text{-}O}$ (Å)	$d_{N\text{-}H}$ (Å)	$\alpha_{N\text{-}O\text{-}H}$ (degrees)	$d_{N\text{-}O}$ (Å)	$d_{O\text{-}H}$ (Å)	$\alpha_{N\text{-}O\text{-}H}$ (degrees)
H	3.564	3.447	75.3	2.620	1.612	10.4
CH_3	3.438	3.261	71.4	2.555	1.633	16.2
tBu	3.600	3.441	72.8	2.561	1.632	16.1
CH_2CHCH_2	3.670	3.530	74.1	2.610	1.596	10.6
$COCH_3$	3.652	3.502	73.4	2.580	1.673	15.6
NO_2	3.235	2.990	66.7	2.669	1.701	10.2

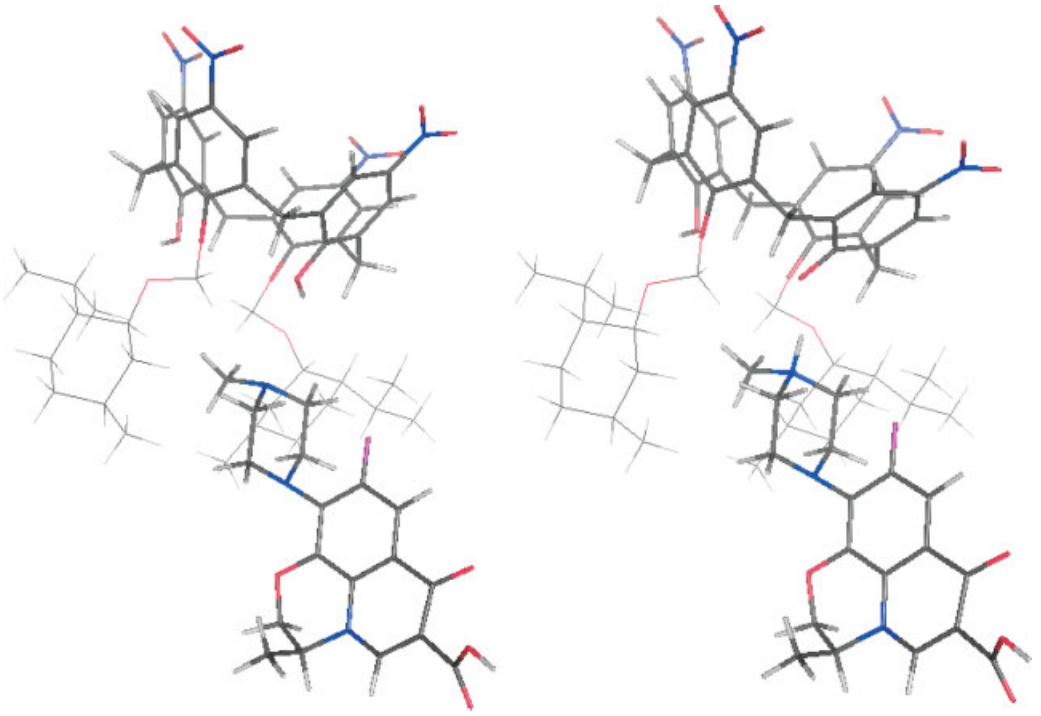

Figure 6. Optimized structures for the neutral (left) and ionized (right) complexes formed by the nitro derivative of the calix[4]arene in Fig. 2 and levofloxacin using the PM3 method

Table 6. The PM3 energies[a] for the interaction between the calix[4]arene derivatives shown in Fig. 2 and levofloxacin in DMSO solution ($\varepsilon = 47$)

	Solution ($\varepsilon = 47$)		
R	Neutral complex	$CalixO^- + HL^{+b}$	Ionized complex[b]
H	−2.65	60.33	13.16
CH_3	−1.27	62.11	16.76
tBu	−0.92	64.98	17.95
CH_2CHCH_2	−2.67	63.09	17.38
$COCH_3$	−1.60	51.43	6.67
NO_2	2.18	32.79	−2.52

[a] Values (in kcal mol^{-1}) are relative to the separated neutral molecules.
[b] The correction in Eqn (7) is applied.

nitro derivative with Lfx. We use the PM3 optimized geometries because optimization at the DFT level is beyond our computational capabilities. The calculations are carried out in the gas phase. At the PM3 level the energy difference (ionized minus neutral form) amounts to 32.54 kcal mol^{-1}, the corresponding value at the DFT level is 9.30 kcal mol^{-1}. Therefore, the PM3 result overestimates this quantity by 23.24 kcal mol^{-1}, in very good agreement with the correction proposed in Eqn (7).

The following remarks can be made concerning the energy values in Table 6. First, the neutral complexes are slightly more stable than the separated molecules except in the case of NO_2, which exhibits a positive relative energy (stabilization of the neutral complexes requires some additional explanation because no hydrogen bonds

are present in this case; we shall come back to this point below). Second, the separated ions are much less stable than the separated neutral molecules. This was also found in the case of model systems but the energy differences are substantially greater in this case (note that values in Table 6 have been corrected by Eqn (7) whereas values in Table 4 were not). The main reason is that the size of the ions is much larger in the present case and therefore they are less stabilized by solute–solvent interactions. It is also interesting to note that NO_2 exhibits a particular behavior because the relative energy of the separated ions is much lower than that found for the other substituents. A significant charge transfer from the phenolate oxygen atom to the NO_2 group is found, which raises the interaction with the solvent (the Mulliken population of the phenolate oxygen changes from -0.619 in the unsubstituted calixarene–Lfx complex to -0.578 in the NO_2-substituted complex). Finally, if one considers the relative energies for the ionized complexes, the corrected PM3 results suggest that this mode of interaction would be favorable in the case of the nitro group only.

As mentioned above, Nachtigall *et al.*[62] have shown that non-substituted calix[4]arene and piperazine molecules form *exo*-ionized complexes in acetonitrile solution. According to our results, ionized complexes are not expected for the calix[4]arene considered here when R = H (corrected relative energy 13.16 kcal mol^{-1}). The (+)-isomenthyl group in the lower rim interacts repulsively with the guest molecule, making the formation of a complex more difficult. However, further computations show that if the isomenthyl groups are removed from the calix[4]arene, then neutral and ionic complexes are indeed predicted with the piperazine molecule (relative energies of -2.53 and -1.63 kcal mol^{-1}, respectively).

A final remark needs to be made. In PM3 calculations, some additional errors may be introduced due to unphysical H–H stabilizing interactions[65], which produce an artificial reduction of the steric hindrance of bulky groups. Such an interaction manifests itself by the presence of H–H distances that are too short after geometry optimization ($\sim$1.7 Å) and indeed we have found some interactions of this kind in the calix[4]arene molecule and in the calix[4]arene–Lfx complexes. Note that this difficulty cannot be solved with the ONIOM methodology.[67] It has been proposed that the original core–core interactions in PM3 should be modified by a parameterized function exhibiting the correct physical behavior[67] and this has been applied to the study of hydrated systems with encouraging results.[68] Recently, a set of parameters for describing interactions between any two molecules containing H, C, N and O atoms has also been reported.[69] We have made some tests of this new core–core parameter set for our host—guest systems and, although improved results are obtained with respect to standard PM3, further developments of the approach appear to be necessary.

CONCLUSION

In this paper, we have clearly shown that PM3 exhibits a systematic error of 24 kcal mol^{-1} in the prediction of ionization processes for phenol/piperazine-related systems. Hydrogen bonds are also a little underestimated. For the calix[4]arene–Lfx compounds considered, it has been shown that the substituents at the upper and lower rims play a crucial role in determining the interaction mode. Without the isomenthyl groups at the lower rim, the formation of neutral and ionized complexes seems possible for unsubstituted calix[4]arene at the upper rim. With the isomenthyl groups at the lower rim, stable complexes should be formed only for strong electron-withdrawing groups such as NO_2. These complexes should exhibit zwitterionic character. In the other cases PM3 predicts a slight stabilization of neutral complexes, but this seems to be due to well-known artifacts of the method. Indeed, no hydrogen bonds are predicted for those structures. The analysis presented in this work, and in particular the comparison with DFT methods for model systems, has allowed us to propose a low-cost computational strategy that can be quite useful for the study of other host–guest systems. Nevertheless, the drawbacks of the PM3 method are also evident and we think that further efforts to improve semi-empirical methodologies would be extremely valuable in this research domain.

Acknowledgment

The authors acknowledge the CNRS center CINES (Montpellier, France) for computational facilities (Project lct2316).

REFERENCES

1. Lesher GY, Froelich EJ, Gruett MD, Bailey RP, Brundage RP. *J. Med. Pharm. Chem.* 1962; **5**: 1063–1068.
2. Monk JP, Campolina Richards DM. *Drugs* 1987; **33**: 346–391.
3. Ernst ME, Ernst EJ, Klepser ME. *Am. J. Health Syst. Pharm.* 1997; **54**: 2569.
4. Hooper DC. *Biochim. Biophys. Acta* 1998; **1400**: 45–61.
5. Hooper DC. *Drugs* 1999; **58**: 6–10.
6. Ball P. *J. Antimicrob. Chemother.* 2000; **46**: 17–24.
7. Davis R, Bryson HM. *Drugs* 1994; **47**: 677–700.
8. Hayakawa I, Atarashi S, Yokohama S, Imamura M, Sakano K, Furukawa M. *Antimicrob. Agents Chemother.* 1986; **29**: 163–164.
9. Horimai T, Ohara M, Ichinose M. *J. Chromatogr. A* 1997; **760**: 235–244.
10. Horstkotter C, Blaschke G. *J. Chromatogr. B* 2001; **754**: 169–178.
11. De Boer T, Mol R, De Zeeuw RA, De Jong GJ, Ensing K. *Electrophoresis* 2001; **22**: 1413–1418.
12. Awadallah B, Schmidt PC, Wahl MA. *J. Chromatogr. A* 2003; **988**: 135–143.
13. Asfari Z, Boehmer V, Harrowfield J, Vicens J. *Calixarenes 2001*, Kluwer Academic: Dordrecht, 2001.
14. Lynam C, Jennings K, Nolan K, Kane P, McKervey M, D. D. *Anal. Chem.* 2002; **74**: 59–66.
15. Zheng Y-S, Zhang C. *Org. Lett.* 2004; **6**: 1189–1192.

16. Grady T, Harris SJ, Smyth MR, Diamond D, Hailey P. *Anal. Chem.* 1996; **68**: 3775–3782.
17. Regnouf-de-Vains J-B, Lamartine R, Fenet B. *Helv. Chim. Acta* 1998; **81**: 661–668.
18. Molard Y, Bureau C, Parrot-Lopez H, Lamartine R, Regnouf-de-Vains J-B. *Tetrahedron Lett.* 1999; **40**: 6383–6387.
19. Ben Salem A, Regnouf-de-Vains J-B. *Tetrahedron Lett.* 2001; **42**: 7033–7036.
20. Guo W, Wang J, Wang C, He J-Q, Cheng J-P. *Tetrahedron Lett.* 2002; **43**: 5665–5667.
21. Lazzarotto M, Sansone F, Baldini L, Casnati A, Cozzini P, Ungaro R. *Eur. J. Org. Chem.* 2001; 595–602.
22. Grootenhuis PDJ, Kollman PA, Groenen LC, Reinhoudt DN, van Hummel GJ, Ugozzoli F, Andreetti GD. *J. Am. Chem. Soc.* 1990; **112**: 4165–4176.
23. Guilbaud P, Varnek A, Wipff G. *J. Am. Chem. Soc.* 1993; **115**: 8298–8312.
24. Fisher S, Grootenhuis PDJ, Groenen LC, van Hoorn WP, van Veggel FCJM, Reinhoudt DN, Martin K. *J. Am. Chem. Soc.* 1995; **117**: 1611–1620.
25. Thondorf I, Brenn J. *J. Mol. Struct. (Theochem)* 1997; **398/399**: 307–314.
26. van Hoorn WP, Briels WJ, van Duynhoven JPM, van Veggel FCJM, Reinhoudt DN. *J. Org. Chem.* 1998; **63**: 1299–1308.
27. Thondorf I. *J. Chem. Soc., Perkin Trans. 2* 1999; 1791–1796.
28. Fraternali F, Wipff G. *J. Incl. Phenom.* 1997; **28**: 63–78.
29. Wipff G. In *Calixarenes 2001*, Asfari Z, Boehmer V, Harrowfield J, Vicens J (eds). Kluwer Academic: Dordrecht, 2001; 312–333.
30. Brouwer EB, Enright GD, Ratcliffe CI, Ripmeester JA, Udachin KA. In *Calixarenes 2001*, Asfari Z, Boehmer V, Harrowfield J, Vicens J (eds). Kluwer Academic: Dordrecht, 2001; 296–311.
31. Lipkowitz KB, Pearl G. *J. Org. Chem.* 1993; **58**: 6729–6736.
32. Li Y, Zeng YZ, Guo JL, Song XQ. *Chem. Lett.* 1994; **5**: 781–784.
33. Bernardino RJ, Costa Cabral BJ, Pereira JLC. *J. Mol. Struct. (Theochem)* 1998; **455**: 23–32.
34. Brouyère E, Bredas JL. *Synth. Met.* 1995; **71**: 1699–1700.
35. Brouyère E, Persoons A, Brédas JL. *J. Phys. Chem. A* 1997; **101**: 4142–4148.
36. Lara-Ochoa F, Cogordan JA, Cruz R, Martinez M, Silaghi-Dumitrescu I. *Fullerene Sci. Technol.* 1999; **7**: 411–419.
37. Golebiowski J, Lamare V, Martins-Costa MTC, Millot C, Ruiz-Lopez MF. *Chem. Phys.* 2001; **272**: 47–59.
38. Chung TD, Kang SK, Kim J, Kim H-S, Kim H. *J. Electroanal. Chem.* 1997; **438**: 71–78.
39. Choe J-I, Kim K, Chang S-K. *Bull. Korean Chem. Soc.* 2000; **21**: 465–470.
40. Bernardino RJ, Costa Cabral BJ. *J. Phys. Chem. A* 1999; **103**: 9080–9085.
41. Bernardino RJ, Costa Cabral BJ. *J. Mol. Struct. (Theochem)* 2001; **549**: 253–260.
42. Hay BP, Nicholas JB, Feller D. *J. Am. Chem. Soc.* 2000; **122**: 10083–10089.
43. Macias AT, Norton JE, Evanseck JD. *J. Am. Chem. Soc.* 2003; **125**: 2351–2360.
44. Golebiowski J, Lamare V, Ruiz-Lopez MF. In *Calixarenes 2001*, Asfari Z, Boehmer V, Harrowfield J, Vicens J (eds). Kluwer Academic Publishers: Dordrecht, 2001; 334–345.
45. Svensson M, Humbel S, Froese RDJ, Matsubara T, Sieber S, Morokuma K. *J. Phys. Chem.* 1996; **100**: 19357–19363.
46. O'Malley PJ. *J. Am. Chem. Soc.* 1998; **120**: 11732–11737.
47. Rinaldi D, Bouchy A, Rivail J-L, Dillet V. *J. Chem. Phys.* 2004; **120**: 2343–2350.
48. Frisch MJ, Trucks GW, Schlegel HB, Scuseria GE, Robb MA, Cheeseman JR, Zakrzewski VG, Montgomery JA, Stratmann RE, Burant JC, Dapprich S, Millam JM, Daniels AD, Kudin KN, Strain MC, Farkas O, Tomasi J, Barone V, Cossi M, Cammi R, Mennucci B, Pomelli C, Adamo C, Clifford S, Ochterski J, Petersson GA, Ayala PY, Cui Q, Morokuma K, Malick DK, Rabuck AD, Raghavachari K, Foresman JB, Cioslowski J, Ortiz JV, Baboul AG, Stefanov BB, Liu G, Liashenko A, Piskorz P, Komaromi I, Gomperts R, Martin RL, Fox DJ, Keith T, Al-Laham MA, Peng CY, Nanayakkara A, Gonzalez C, Challacombe M, Gill PMW, Johnson B, Chen W, Wong MW, Andres JL, Gonzalez C, Head-Gordon M, Replogle ES, Pople JA. *Gaussian 98, Revision A.11.3*. Gaussian: Pittsburg, PA, 1998.
49. Weiner SJ, Kollman PA, Case DA, Singh UC, Ghio C, Alagona G, S. PJ, Weiner P. *J. Am. Chem. Soc.* 1984; **106**: 765–784.
50. Gutsche CD, Iqbal M, Alam I. *J. Am. Chem. Soc.* 1987; **109**: 4314–4320.
51. Bauer LJ, Gutsche CD. *J. Am. Chem. Soc.* 1985; **107**: 6063–6069.
52. Arena G, Contino A, Gulino FG, Magri A, Sansone F, Sciotto D, Ungaro R. *Tetrahedron Lett.* 1999; **40**: 1597–1600.
53. Nachtigall FF, Vencato I, Lazzarotto M, Nome F. *Acta Crystallogr.* 1998; **C54**: 1007–1010.
54. Brouwer EB, A. UK, Enright GD, Ripmeester JA. *Chem. Commun.* 2000; 1905–1906.
55. Thuéry P, Asfari Z, Nierlich M, Vicens J. *Acta Crystallogr.* 2002; **C58**: 0223–0225.
56. Mohammed-Ziegler I, Poór B, Kubinyi M, Grofcsik A, Grün A, Bitter I. *J. Mol. Struct.* 2003; **650**: 39–44.
57. Ghoufi A, Bonal C, Morel JP, Morel-Desrosiers N, Malfreyt P. *J. Phys. Chem. B* 2004; **108**: 5095–5104.
58. Harrowfield JM, Ogden MI, Richmond WR, Skelton BW, White AH. *J. Chem. Soc., Perkin Trans. 2* 1993; 2183–2190.
59. Harrowfield JM, Richmond WR, Sobolev AN. *J. Incl. Phenom.* 1994; **19**: 257–276.
60. Danil de Namor AF, Cleverley RM, Zapata-Ormachea ML. *Chem. Rev.* 1998; **98**: 2495–2525.
61. Shinkai S, Araki K, Grootenhuis PDJ, Reinhoudt DN. *J. Chem. Soc., Perkin Trans. 2* 1991; 1883–1886.
62. Nachtigall FF, Lazzarotto M, Nome F. *J. Braz. Chem. Soc.* 2002; **13**: 295–299.
63. Berthalon S. *Thesis*, University Claude Bernard-Lyon 1, France, 1998.
64. Fu Y, Liu L, Li R-Q, Liu R, Guo Q-X. *J. Am. Chem. Soc.* 2004; **126**: 814–826.
65. Buss V, Messinger J, Heuser N. *QCPE Bull.* 1991; **11**: 5–7.
66. Casadeus R, Moreno M, Gonzales-Lafont A, Lluch JM, Repasky MP. *J. Comp. Chem.* 2004; **25**: 99–105.
67. Bernal-Uruchurtu MI, Martins-Costa MTC, Millot C, Ruiz-Lopez MF. *J. Comp. Chem.* 2000; **21**: 572–581.
68. Harb W, Bernal-Uruchurtu MI, Ruiz-Lopez MF. *Theor. Chem. Acc.* 2004; **112**: 204–216.
69. Harb W. *PhD Thesis*, Université Henri Poincaré, Nancy I, France, 2004.